Tensile Strength of Embedded Anchor Groups: Tests and Strength Models

DAVID A. GRILLI and AMIT M. KANVINDE

ABSTRACT

Steel column bases in seismically braced frames and other similar structures must be designed for high uplift or tensile forces. A common detail for this connection involves anchors embedded in the footing with a plate at their lower end, also embedded in the footing. This detail is increasingly prevalent in construction practice because it is exempt from the strength calculations of ACI 318 Appendix D. However, no experimental data or validated design guidelines are available to support the design of this detail. As a consequence, approaches from other similar situations (such as punching shear of slabs) are adapted for this purpose. To address this practical need, this paper presents tension tests on two full-scale specimens featuring this anchorage detail. The main variable examined in the experiments is the embedment depth, such that two depths (12 and 18 in.) are tested. The test specimens exhibit a classic concrete failure cone extending upward from the edges of the embedded base plate. The experimental data provide evidence that the anchorage detail provides an effective means to carry high-tensile loads. The data are evaluated against three strength models, including the ACI 318 Appendix D method, the ACI 318 punching shear equation and the concrete capacity design (CCD) method. It is determined that the ACI 318 Appendix D method is significantly conservative (average test-predicted ratio of 1.34) because it does not consider the beneficial effects of the embedded plate. On the other hand, the punching shear method has an average test-predicted ratio of 0.62. The CCD method shows the most promise, with an average test-predicted ratio of 0.99. Limitations of the study include the small size of the test set and the minimal reinforcement in the specimens.

Keywords: anchorages; base connections.

INTRODUCTION

Column bases in steel frames (particularly braced frames) must often be designed for high-tensile (i.e., uplift) forces. These forces may be a result of overturning moments induced by high-seismic or -wind events or, in the case of concentrically based frames, for the development of the tensile capacity of diagonal braces as required by current steel design provisions (AISC, 2010). Various detailing alternatives are available for transferring this tensile force from the steel column into the concrete footing below. Figures 1a and b show two such details that are commonly used in current construction practice.

Figure 1a shows a detail that uses individual, standard-headed anchors or anchor rods with nuts at the embedded ends. While convenient to fabricate, these details are problematic if large tensile loads (i.e., >50 kips or so) must be resisted for the following reasons: (1) The strength is

calculated in accordance with ACI 318-14 Appendix D (ACI, 2014) as the group capacity based on individual, standard-headed anchor bolts or nutted anchor rods. In many cases, the embedment depth or number of anchor rods required by this provision becomes impractical. (2) There is an apparent dichotomy wherein the strength calculation of a similar detail for reinforced concrete columns with hooked reinforcement bars extending into the footing is not subject to ACI 318 Appendix D requirements; only the rebar tensile strength is checked. This results in strength estimates that are significantly higher than those determined as per ACI 318 Appendix D.

In response to these issues, designers often employ a detail similar to that shown in Figure 1b. This detail resists uplift force through a single plate embedded at the lower end of the anchor bolts. This detail will typically include supplemental reinforcement around the embedded plate. This detail is attractive to designers because the provisions of ACI 318 Appendix D explicitly state that such a detail is outside its scope. Specifically, referring to ACI 318 D.2.2:

> Specialty inserts, through-bolts, multiple anchors connected to a single steel plate at the embedded end of the anchors, grouted anchors, and direct anchors such as powder or pneumatic actuated nails or bolts are not included in the provisions of Appendix D.

The detail shown in Figure 1b circumvents the provisions of Appendix D. However, Appendix D (or any other design

David A. Grilli, Graduate Research Assistant, Department of Civil and Environmental Engineering, University of California, Davis, CA. Email: dagrilli@ucdavis.edu

Amit M. Kanvinde, Professor, Department of Civil and Environmental Engineering, University of California, Davis, CA (corresponding). Email: kanvinde@ucdavis.edu

standard) does not provide a method for the design of such a detail, with the implication that either engineering judgment must be used or alternative design provisions must be adapted for design. These alternatives include the current ACI provisions for punching shear (ACI 318, Chapter 11) or bearing capacity (ACI 318, Chapter 10) of concrete members. At first glance, these situations (i.e., the embedded plate details and punching shear/bearing) appear similar. However, there are subtle differences in physical response between these situations and the anchorage details such as the one shown in Figure 1b. Specifically, these pertain to (1) the reinforcing of the footing with respect to the embedded plate, (2) installation of the embedded plate itself (i.e., if the embedded plate needs to be cast in a protective lean mix below the bottom of footing prior to the footing pour, such that the plate is actually bearing against a cast surface rather than cast within the footing) and (3) size effects in concrete (i.e., the embedment of these connections is often larger than seen in slab/punching shear situations, and thus these may be weaker on a unit basis as compared to situations for which the punching shear approaches have been developed). In the absence of guidance for the design of these anchorages in ACI 318 or any other design codes and the absence of test data that demonstrate their strength and response, engineers and review agencies are often required to make design choices that are expensive and possibly conservative (e.g., requiring the plate to be positioned such that it bears on the bottom of the concrete footing).

Motivated by these problems, this paper presents results on two full-scale tests on anchorage details similar to the ones shown in Figure 1b. The primary objectives of this study are as follows:

1. To develop fundamental understanding of the failure modes and force transfer mechanisms in anchor group details subjected to tension uplift, based on large-/full-scale experimental data.

2. To develop, validate and establish design provisions for these details that are otherwise specifically excluded from ACI 318 Appendix D.

3. To demonstrate details that can economically achieve design strength for high uplift forces.

This paper describes two full-scale experiments conducted to accomplish these objectives. The next section describes the experiments and presents their results relative to commonly used strength prediction models. The paper concludes by summarizing possible design methods.

EXPERIMENTAL PROGRAM

Two large-scale experiments were conducted to realize the objectives of the study. The primary variable considered was the embedment depth, d_{embed}, indicated schematically in Figure 1b. In this study, two embedment depths were considered—that is, d_{embed} = 12 and 18 in. Figure 2 shows a photograph of the test setup and specimen prior to testing, whereas Figure 3 schematically shows various detailing/reinforcement aspects of the specimens. The photograph in Figure 2 shows test 1; the test specimen for test 2 appears identical—the only difference is in the embedment depth.

Test Setup

Referring to Figures 2 and 3, the key aspects of the test setup are as follows:

1. Both specimens featured blocks that measured 40 in. (height) × 140 in. × 108 in. The large size of the block was necessitated by the following considerations:
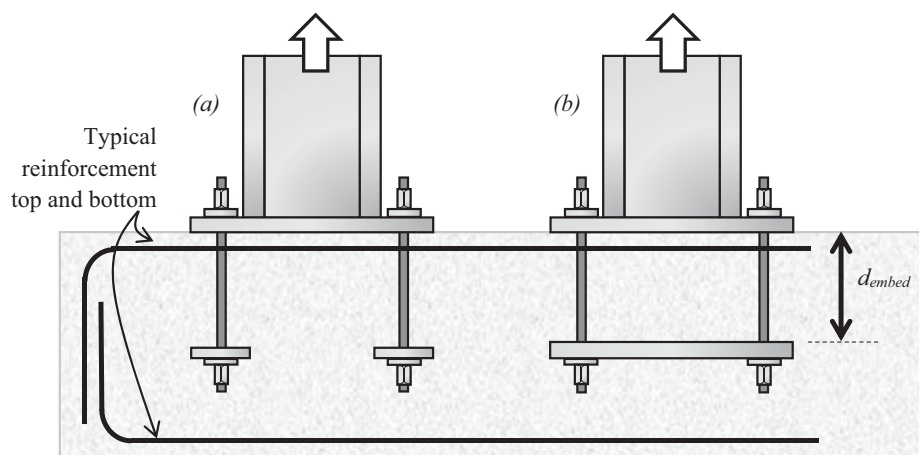

Fig. 1. (a) Base connection with individual anchors; (b) base connection with anchors connected to an embedded plate.
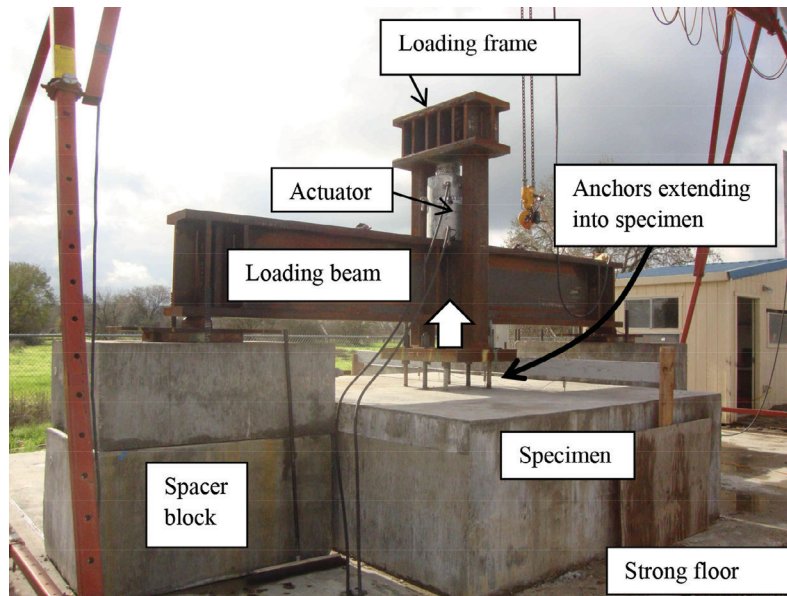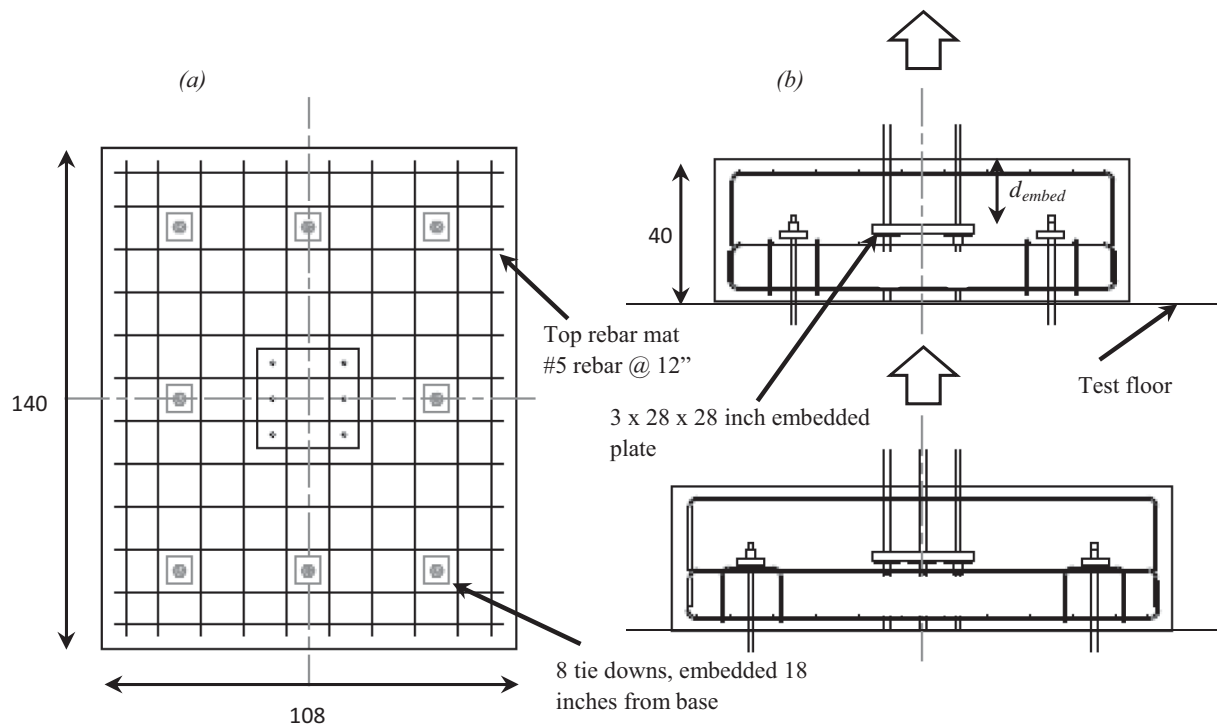
Fig. 2. Photograph of test setup.

Fig. 3. Specimen details: (a) plan; (b) two elevations.

a. In plan, the large dimension was necessary to ensure that the failure cone was fully accommodated within the footing, thereby avoiding edge effects. In fact, the size of the block was large enough that the zones of compressive stress induced by the tie-down rods (shown in Figure 3b) had minimal effect on the possible failure cone.

b. In elevation, a key consideration was to ensure that the underside of the specimen (i.e., below the applied load) was anchored to the strong floor such that failure of the footing did not occur due to bending. An especially important consideration here is that experimental strength for pure tensile failure is relatively unaffected by boundary conditions.

2. Following from point 1, the anchor system was elaborately designed with two considerations, with competing effects: (a) spacing the outside anchors as far out as possible to minimize interaction with the failure cone and (b) including anchors in the line of action of the loads to preclude bending of the block. This latter consideration was realized by installing tie-downs projecting upward from the strong floor over which the specimen was cast in place. These tie-downs (whose locations are shown in Figure 3) had an embedded plate attached to their top surface to enable engagement with the specimen.

3. The loading apparatus, as shown in Figure 2, included a cross beam and a frame between which a hydraulic cylinder actuator (with 1,000-kip capacity) was inserted such that the loading frame could be lifted up. A 4-in. plate was attached to the lower surface of the loading frame. Six anchor rods attached to this plate were embedded in the concrete and attached to the embedded plate, which in turn exerted the uplift forces on the concrete. The embedded plates were identical in both test specimens, and measured 3 in. × 28 in. × 28 in. (the plate was sized to remain elastic under the applied loads). The anchor rods were A722 Grade 150 rods of 1⅜-in. diameter and designed to remain elastic during the loading.

4. Reinforcement was provided in the top layer. This consisted of a light rebar mat, which consisted of #5 rebar with a spacing of 12 in. The reinforcement was used to provide minor resistance against uplift as well as to mitigate surface cracking. No vertical reinforcement was provided. The main purpose of this was to isolate the effect of the concrete resistance in a clean way such that it would be transferable to design situations with varying reinforcement wherein the contribution of reinforcement is addressed separately. A systematic study of the effect of reinforcement is possible through additional testing, which varies the reinforcement as a test parameter.

5. Both specimens were cast on the same day, although tested on different days. Test 1 was tested on day 28 with respect to the pour, whereas test 2 was tested on day 31. Standard test cylinders were taken from each of these pours to measure the compressive strength of concrete f'_c; results from these ancillary tests are presented in a subsequent section.

6. The specimens were all loaded monotonically, with an approximate rate of 1 kip per second.

Test Instrumentation

The load in the specimens was monitored using a pressure gage. As a secondary measurement of load, a linear strain gage was attached to the top surface of the loading beam, which remained elastic throughout the loading. Displacement transducers were affixed to three locations on the top surface of the concrete as well as to the top plate to measure upward displacement of the loading frame. A camera was suspended directly above the test setup to capture crack formation in the entire block. Another camera captured an elevation (profile) view of the test to observe vertical displacements of the test equipment and concrete failure cone. Based on these instruments, a load deformation curve was generated, results of which are discussed in a subsequent section.

Ancillary Tests

Six standard, 6-in. × 12-in. concrete cylinder samples were collected and tested at the 28-day cure mark. For the construction of the specimen blocks, a total of three trucks were required, and two samples from each truck were tested. The analysis of test data relative to the models (discussed in a subsequent section) is based on the average value of $f'_c = 4,336$ psi (standard deviation of 282 psi) for the cylinder samples for each test. The low standard deviation suggests a relatively uniform strength throughout the specimen block. The weight density of the various samples was (on average) 145 lb/ft^3, which is consistent with plain structural concrete used in practice.

Test Results

Load-displacement curves for both experiments are shown in Figure 4. Peak loads (denoted P_{test}^{max} and also shown on the figure) are summarized in Table 1. Both tests showed similar response, wherein little physical damage was observable in the initial elastic region of loading. Failure was observed

Table 1. Test Results and Comparison with Strength Prediction Methods				
d_{embed} (in.)	P_{test}^{max} (kips)	Test-to-Predicted Ratios		
		$P_{test}^{max}/P_n^{ACI318-D}$	P_{test}^{max}/P_n^{PS}	P_{test}^{max}/P_n^{CCD}
12	317	1.29 (1.58)*	0.65	0.92 (1.13)†
18	495	1.39 (1.61)*	0.59	1.07 (1.21)†
Mean		1.34 (1.60)*	0.62	0.99 (1.17)†
Coefficient of Variation		0.05 (0.01)*	0.07	0.11 (0.05)†

* Value in parentheses calculated without considering increase in perimeter of projected area due to plate thickness as allowed by (ACI 318, D.5.2.8).
† Value in parentheses calculated by excluding area of plate from projected area.

in the form of (1) a sudden drop in load, (2) appearance of a crack on the top surface of the concrete, and (3) a lifting of the "failure cone" by approximately 2 in. The failure of test 2, with d_{embed} = 18 in., was somewhat more sudden as compared to that of test 1. Other than the concrete failure, all components in the setup (i.e., anchors, embedded plate, loading beam) remained elastic as designed.

Figures 5a and b show post-test photographs of tests 1 and 2 taken from a high angle above the specimens, illustrating the entire failure surface after the loading beam had been removed. Figures 6a and b show similar profile photographs, illustrating the uplift of the concrete cone. Based on the location of this crack, an inferred profile of the failure cone is illustrated schematically in Figures 7a and b. Referring to the figures and physical measurements of the failure cone, the approximate angle of the failure cone surface with respect to the horizontal is 28° for test 1 and 33° for test 2.

STRENGTH MODELS

Referring to the introductory discussion, a major objective of this paper is to provide support for the development of strength characterization approaches for these anchorages. Accordingly, three strength characterization approaches are evaluated against the test data. These are (1) the ACI 318 Appendix D approach for the breakout strength of anchor groups, (2) the ACI 318 Chapter 11 punching shear equation and (3) the concrete capacity design (CCD) approach proposed by Fuchs et al. (1995). The first two are selected based on their prevalence in design practice, whereas the third is selected based on its promise in characterizing the strength of a large variety of concrete embedments and fastenings, as shown by previous studies (e.g., Gomez et al., 2009). Each of these methods is now briefly described, and the resulting strength estimates are compared to test data.

Method 1

ACI 318 Appendix D provides the following equation (which has been adapted to the current test parameters) to predict the breakout strength of an anchor group in concrete (loaded concentrically, cast-in anchors, no edge effects):

$$P_n^{ACI318-D} = \frac{A_{Nc}}{A_{Nco}} \times \psi_{c,N} \times N_b \qquad (1)$$
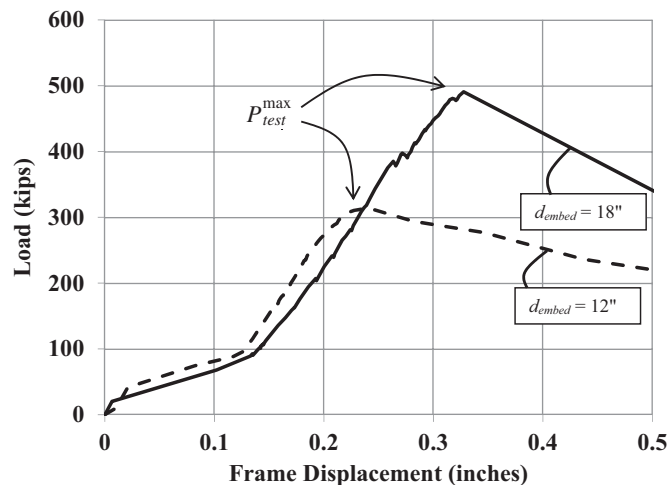
Fig. 4. Load deformation curves of the two specimens.

Fig. 5. Overhead view of breakout surface: (a) 12-in. embedment; (b) 18-in. embedment.

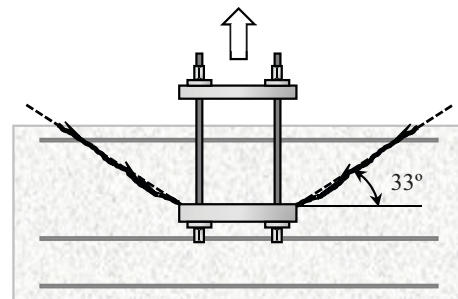Fig. 6. Profile view of breakout surface: (a) 12-in. embedment; (b) 18-in. embedment.
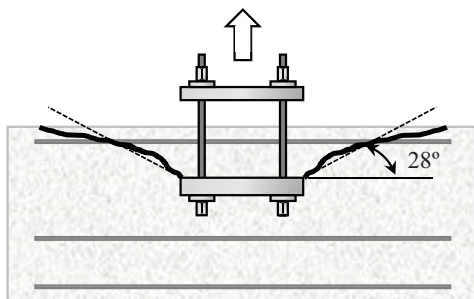

Fig. 7. Schematic illustration of breakout cone: (a) 12-in. embedment; (b) 18-in. embedment.

where, for 11 in. $< d_{embed} <$ 23 in.,

$$N_b = 16 \times \sqrt{f_c'} \times d_{embed} \qquad (2)$$

and

A_{Nc} = projected concrete failure area of a group of anchors, in.^{2}

A_{Nco} = projected concrete failure area of a single anchor, in.^{2}

$\psi_{c,N}$ = 1.25 for cast-in anchors without cracking at service loads

This method was derived based on both the tensile capacity of concrete and fracture mechanics concepts. The projected area is defined by projecting planes from the anchorage depth to the free surface at 35° angles. Modification factors are used when the planes intersect free-side surfaces. This method is based on experimental data on embedded single anchors and anchor groups (Klingner et al., 1982; Cook and Klingner, 1992; Fuchs et al., 1995; Farrow and Klingner, 1995; Zhang et al., 2001; Anderson and Meinheit, 2005; Eligehausen et al., 2006; Lee et al., 2007; Ožbolt et al., 2007) and, as a result, is accurate for deeply embedded single anchors and anchor groups. For the same reason, this approach cannot account for the favorable effects of connecting the embedded anchors to a common plate. In fact, the strength estimate implied by Equation 1 is identical to the calculations that would result from considering the anchor group without a plate present. It may be argued that this is conservative because it does not account for (1) the larger bearing area of the concrete that may delay fracture initiation and (2) a greater degree of confinement in the concrete above the plate. While the method does not explicitly account for the plate as a bearing surface, the plate may be considered effective as a washer to determine the location from which the failure surface originates (per provision D.5.2.8 of the Appendix). Per this provision, the effective dimension of this plate or washer may be considered equal to the thickness of the attached plate (3 in. in this case).

Method 2

ACI 318 Chapter 11 provides provisions for punching shear to be used in the case where a column exerts a vertical load on a reinforced concrete slab. As discussed in the introductory remarks, this method is sometimes used for anchorage design because the modes of failure appear to be similar. Using this approach, the applicable equation is

$$P_n^{PS} = 4 \times \sqrt{f_c'} \times b_0 \times d_{embed} \qquad (3)$$

The equations have been greatly simplified for ease of design and are based on fitting to experimental data (ACI-ASCE, 1962). Strength predictions are based on the depth

of the slab, concrete material properties and a "critical section" based on the loading area and depth of the slab. The formulation is intended to reduce the dependency of strength on ratio of column size to slab depth. The critical section is defined as the area that minimizes the perimeter a minimum while maintaining a distance of $d_{embed}/2$ to the edges or corners of the column or loading area. This may be interpreted to imply that failure occurs when a tensile stress of $4 \times \sqrt{f_c'}$ is reached over the projected area of a 45° failure cone emanating from the edges of the embedded plate. For the particular geometry of the specimens used in this study, b_0 may be calculated using the following equation:

$$b_0 = 4 \,(28 \text{ in.} + d_{embed}) \qquad (4)$$

However, a closer inspection of the sources (ACI-ASCE, 1962) used to formulate this approach reveal two interesting factors. First, it does not explicitly incorporate fracture mechanics or the "size effect" in concrete (Bažant, 1984), which implies that the unit strength (or failure stress) of geometrically self-similar concrete components varies inversely with their size because failure is controlled by localized fracture rather than by large-scale yielding. The presence of reinforcement mitigates this effect by distributing deformations. Second, this equation is based on 198 tests on concrete slabs that were reinforced and included a large set of data on slabs thinner than 10 to 12 in. When considered together, these two points present an obvious challenge in extrapolating the equation to the anchorages tested, which have significantly deeper embedment and are also dissimilar physically as compared to a concrete column on a slab.

Method 3

Another approach, which explicitly considers the size effect, is based on a method originally proposed Fuchs et al., (1995). This method, referred to as the concrete capacity design (CCD) method has been demonstrated to characterize concrete failure strength for a wide variety of fastenings, including shear lugs (Gomez et al., 2009). In fact, the method used in ACI-318 Appendix D is partially based on the CCD method. The nominal breakout capacity of concrete for cast-in anchors as derived in the CCD method, adapted to the conditions of the tests, can be reduced to the following equation:

$$P_n^{CCD} = \frac{1}{\sqrt{d_{embed}}} \times \left(\frac{40}{9}\right) \times \sqrt{f_c'} \times A_{Nc} \qquad (5)$$

where A_{Nc} refers to the projected area assuming a 35° breakout cone, shown schematically in Figure 8.

Referring to Equation 5, the term $\sqrt{d_{embed}}$ in the denominator of the right-hand side of the equation may be interpreted as a modifier that explicitly incorporates the size effect such that the effective tensile stress capacity (or unit

strength) of the concrete is diminished as the embedment depth increases. The square root dependence of the effective stress may be determined directly from fracture mechanics concepts (Anderson, 1995). Another observation is that the area A_{Nc} is different as compared to the area used in the punching shear method (in Equation 3). However, as identified previously (Gomez et al., 2009), the projected area does not bear physical significance to the final breakout surface, which is a result of fracture propagation, but rather may be interpreted as a convenient basis for characterizing the effective stress at which fracture initiation occurs. The projected area may be calculated in two ways—one includes the area of the embedded plate within it, whereas the other excludes it. Inclusion of the area of the embedded plate assumes that the adhesive bond developed between the underside of the plate and the concrete is greater than the concrete tensile strength, whereas the exclusion assumes that no adhesion is present. The effect of these assumptions is discussed in the next section.

DISCUSSION

Test-predicted ratios for the three models are presented in Table 1. Referring to the table, the following observations may be made:

1. The ACI-318 Appendix D method is quite conservative; the test-predicted ratios $P_{test}^{max}/P_n^{ACI318-D}$ are determined to be 1.29 and 1.39 for tests 1 and 2, respectively (average of 1.34). This is an important observation, confirming the concerns about the Appendix D method raised earlier, because it provides empirical evidence that the method may not be economical for designing connections with an embedded plate. It is important to note here that the attached plate in these tests is fairly thick (3 in.). As a result, the use of provision D.5.2.8, which allows the consideration of the plate thickness as an effective washer dimension, significantly adds to the strength. If the strength is calculated without considering this
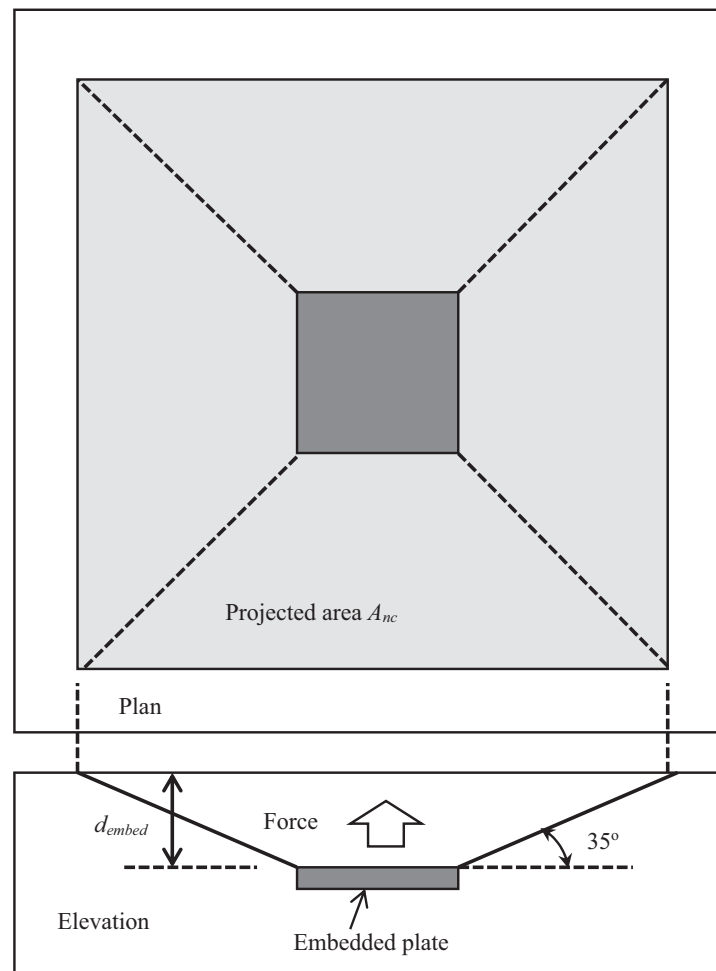

Fig. 8. Effective projected area for CCD method (may or may not include area of plate).

increase in perimeter (i.e., projecting the failure area from the anchor rods), then the conservatism of the ACI method is increased, such that the average test-predicted ratio is 1.60, as indicated in Table 1.

2. For the ACI punching shear method, the test-predicted ratios P_{test}^{max}/P_n^{PS} are 0.65 and 0.59 for tests 1 and 2, respectively, suggesting that when considered relative to other methods (such as the CCD method discussed next), this method may not be optimal for designing the anchorages. A closer inspection of the scientific basis for the punching shear method indicates that it is based on 198 tests of slabs, of which many are thin, compared to the embedment depth of the anchorages. As a result, this observation is not entirely surprising. On the other hand, it is important to note that (a) the current study includes only two experiments, such that the limited size of the study may compromise its statistical significance, and (b) the anchorages are different than a concrete column on a slab.

3. The CCD method appears to be the most accurate of the three methods considered. The test-predicted ratios P_{test}^{max}/P_n^{CCD} are 0.92 and 1.07 for tests 1 and 2, respectively, resulting in an average P_{test}^{max}/P_n^{CCD} value of 0.995. If the area of the plate is excluded from the projected area, the average test-predicted ratio is 1.17, suggesting that significant adhesion may be present between the steel and the concrete. This is consistent with similar results on concrete-steel adhesion by the Federal Highway Administration (FHWA, 2000), through the use of "pull-off" tests that indicate adhesion stresses in the range of 100 to 150 psi, which are greater than the effective tensile stress used in the CCD method.

4. For each of the models, the test-to-predicted ratios are similar for both tests, indicating that the epistemic error introduced by any of the models is not significantly affected by the embedment depth.

It is informative to compare the assumptions underlying the punching shear method and the CCD method because they provide insight into the physical processes controlling failure. Specifically, the punching shear method assumes that the concrete failure strength is directly proportional to the projected area of the 45° cone, with the implication that a uniform tensile stress is mobilized over the failure surface. Research (Bažant, 1984) has shown that this assumption is realistic only when the characteristic specimen dimension (embedment depth in this case) is within 10 to 20 times the aggregate size—that is, approximately 6 to 8 in. For larger components, failure is controlled by fracture mechanics, wherein failure initiates over a smaller area and then propagates as the failure cone. As a result, the effective failure stress (when considered over a projected area) is lower. The CCD method explicitly captures this effect.

SUMMARY AND CONCLUSIONS

Two full-scale experiments were conducted to examine the tensile capacity of anchorage details with anchor bolt groups connected by a plate embedded within a concrete footing. The anchorage type examined in this study is commonly used at the base of columns in braced frames where large uplift forces must be resisted. The tests were motivated by the lack of guidance in design standards for such a detail and by the challenges in adapting design methods originally developed for other types of details.

The main variable interrogated in the experiments was the embedment depth, such that two values—12 and 18 in.—were investigated. The specimens were composed of six anchor rods (1⅜-in. diameter, A722 Grade 150 rods) connected to a 3-in. × 28-in. × 28-in. plate embedded within the concrete. The specimens were designed with minimal reinforcement (to isolate the concrete strength) and were sized to minimize the effect of boundary conditions or specimen bending on the pullout strength. Both tests showed a similar mode of failure with a concrete failure cone emanating at approximately 30° from the edges of the embedded plate.

The specimen strengths were evaluated against three strength characterization approaches. It was found that the concrete capacity design (CCD) method developed by Fuchs et al., (1995) provides excellent agreement with test data. On the other hand, the ACI 318 Appendix D method is significantly conservative, presumably because it does not consider the beneficial effects of the embedded plate.

Finally, it is important to recognize the limitations of this study in interpreting its results. The most obvious limitation is test sample size (i.e., two tests), which was controlled by the physical size and expense of these specimens relative to the budgetary constraints. A consequence of this small sample size is that other variables—such as plate shapes and sizes, anchor rod layouts, edge distances or the use of other embedments instead of a plate (e.g., interconnected channels)—were not examined. Another consequence is that it in the absence of replicate tests, it is difficult to isolate the inherent variability in experimental data from epistemic bias in the models evaluated against the data. As a result, the test data, in itself, cannot be used to calibrate resistance (i.e., ϕ) factors. Moreover, the test specimens did not contain vertical reinforcement. This was a deliberate decision, considering that these experiments are the some of the first of their kind, and intended to establish fundamental, baseline response of the concrete itself. It is anticipated that the presence of reinforcement will increase the strength through two mechanisms: (1) the additional yielding strength provided by

the rebar and (2) the mitigation of the size effect in concrete. An explicit incorporation of these effects will require additional testing, as well as finite element simulation to generalize the results. These are recommended areas for future work.

ACKNOWLEDGMENTS

SYMBOLS

A_{Nc}	Projected concrete failure area of a group of anchors for ACI 318 Appendix D and CCD methods
A_{Nco}	Projected concrete failure area of a single anchor for ACI 318 Appendix D method
b_0	Effective perimeter for the punching shear approach
d_{embed}	Embedment depth; distance from the concrete surface to top surface of the embedded plate
f'_c	Compressive strength of concrete
P_{test}^{max}	Maximum load determined from experiment
$P_n^{ACI318-D}$	Strength estimated as per ACI 318 Appendix D
P_n^{CCD}	Strength estimated as per the CCD approach
P_n^{PS}	Punching shear strength estimated as per ACI 318 Chapter 11
$\psi_{c,N}$	1.25 for cast-in anchors without cracking at service loads for ACI 318 Appendix D method

REFERENCES

ACI (2014), *Building Code Requirements for Structural Concrete and Commentary*, ACI 318-14 and ACI 318R-14, American Concrete Institute, Farmington Hills, MI.

ACI-ASCE (1962), "Shear and Diagonal Tension," *ACI Journal, Proc.* Vol. 59, No. 1, Jan., pp. 1–30; No. 2, Feb., pp. 277–334; and No. 3, Mar., pp. 352–396.

AISC (2010), *Seismic Provisions for Structural Steel Buildings*, AISC 341, American Institute of Steel Construction, Chicago, IL.

Anderson, N.S. and Meinheit, D.F. (2005), "Pryout Capacity of Cast-In Headed Stud Anchors," *PCI Journal*, Vol. 50, No. 2, pp. 90–112.

Anderson, T.L. (1995), *Fracture Mechanics: Fundamentals and Applications*, 2nd ed., Boca Raton, FL: CRC Press.

Bažant, Z.P. (1984), "Size Effect in Blunt Fracture: Concrete, Rock, Metal," *Journal of Engineering Mechanics,* ASCE, Vol. 110, No. 4, pp. 518–535.

Cook, R.A. and Klingner, R.E. (1992), "Behavior of Ductile Multiple-Anchor Steel-to-Concrete Connections with Surface-Mounted Baseplates," *Anchors in Concrete: Design and Behavior,* SP-130, pp. 61–122, American Concrete Institute, Farmington Hills, MI.

Eligehausen, R., Mallée, R. and Silva, J. (2006), *Anchorage in Concrete Construction*, Berlin: Ernst & Sohn (J. T. Wiley).

Farrow, C.B., and Klingner, R.E. (1995), "Tensile Capacity of Anchors with Partial or Overlapping Failure Surfaces: Evaluation of Existing Formulas on an LRFD Basis," *ACI Structural Journal,* Vol. 92, No. 6, pp. 698–710.

Federal Highway Administration (2000), "Tensile Bond Strength of a High Performance Concrete Bridge Deck Overlay," FHWA Project #9904, Project Report, Washington, DC: U.S. Department of Transportation.

Fuchs, W., Eligehausen, R. and Breen, J.E. (1995), "Concrete Capacity Design (CCD) Approach for Fastening to Concrete," *ACI Structural Journal,* Vol. 92, No. 1, pp. 73–94.

Gomez, I.R., Kanvinde, A.M., Smith, C. and Deierlein, G.G. (2009), "Shear Transfer in Exposed Column Base Plates," Technical Report submitted to the American Institute of Steel Construction, Chicago, IL.

Klingner, R.E., Mendonca, J.A. and Malik, J.B. (1982), "Effect of Reinforcing Details on the Shear Resistance of Anchor Bolts Under Reversed Cyclic Loading," *Journal of American Concrete Institute*, Vol. 79, No. 1, pp. 3–12.

Lee, N.H., Kim, K.S., Bang, C.J. and Park, K.R. (2007), "Tensile-Headed Anchors with Large Diameter and Deep Embedment in Concrete," *ACI Structural Journal,* Vol. 104, No. 4, pp. 479–486.

Ožbolt, J., Eligehausen, R., Periškić, G. and Mayer, U. (2007), "3D FE Analysis of Anchor Bolts with Large Embedment Depths," *Engineering Fracture Mechanics,* Vol. 74, pp. 168–178.

Zhang, Y.G., Klingner, R.E. and Graves, H.L. (2001), "Seismic Response of Multiple-Anchor Connections to Concrete," *ACI Structural Journal,* Vol. 98, No. 6, pp. 811–822.